International Journal of Innovative Technology and Exploring Engineering (IJITEE)
ISSN: 2278-3075 (Online), Volume-10 Issue-1, November 2020

A False Positive Decision on the Patient Skin Based on the Statistical Parameters and Visual Quality Measures of Skin Images after Applying Morphological Filters

Sree Hari Raju. S, Rajan. E.G

Abstract: ***This paper is describing about the statistical parameters / boundaries and visual quality proportion of skin pictures in the wake of applying morphological channels. An extraordinary contextual analysis is clarified and executed where a dermatologist settled on a false positive choice on the status of the skin of a patient. This is the most noteworthy aspect of the standard working technique recommended in this paper.***

Keywords: Statistical Parameters, Morphological Filters, Dermatologist, Carcinoma, Texture

I. INTRODUCTION

Skin pictures, which contain skin carcinoma, are outwardly discernible, though skin pictures, which seem typical and smooth don't show any indication of skin carcinoma. In such cases, one needs to handle pictures to remove any shrouded manifestation for carcinoma. Morphological sifting is taken a stab at skin pictures to manage this work. A lot of three skin pictures, which give off an impression of being typical are considered for a total contextual analysis 1. Texturization and morphological handling may help find irregularities in skin pictures that may prompt development of skin carcinoma.

A patient's both ways legs were influenced by parasite and it was expressed that the patient has skin carcinoma in the legs. The shot pictures of both left and right legs are appeared and clarified in contextual analysis 2.

A. Digital Images - Texturization

Spatially rehashed 'Patterns' are alluded as the term called 'texture'. 'Points' are the spatially rehashed designs for a line and a bend. An essential example called 'motif' could be utilized to shape a surface by tiling the motifs in a necessary way. For instance, Fig. 1 shows a texture framed of a particular motif.

Fig. 1: Sample texture formed of a motif

Revised Manuscript Received on November 30, 2020.
***** Correspondence Author
S. Sree Hari Raju*, Research Scholar, Dept. of Computer Science, MG-NIRSA, Affiliated to University of Mysore, Manasagangotri, Mysore, Karnataka, India. E-mail: rvs2raju@gmail.com
Prof. E.G. Rajan, Director, MG-NIRSA. E-mail: rajaneg@yahoo.co.in

Some textures are available on every meaningful picture and can be as directional textures. One has eight directions in a digital lattice as shown in Fig. 2.

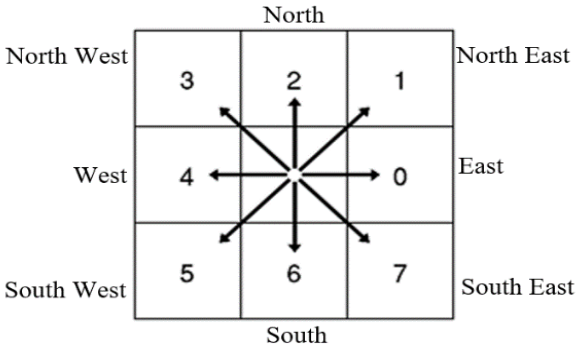

Fig. 2: Digital lattice eight directions

B. Algorithm for Texturization

{
filter the given picture by a 3x3 void window; at each position read picture pixels shrouded in the nine neighborhood; play out the accompanying tasks: (I) think about a reference course, say 'east'; check the focal pixel esteem with pixel in the cell number '0'; if the focal pixel esteem is not as much as incentive in cell number '0' at that point write in an eight digit register (beginning from left) the worth '0', else compose the worth '1'; rehash this system to cell number '1', cell number '2' up to
cell number '7'; the subsequent string in the register will be a paired string; assess what might be compared to this double string and supplant the focal pixel estimation of the picture by this decimal number; rehash this whole method for all pixels in the picture each in turn; the subsequent picture would be the east insightful texturized picture
}

One can get eight texturized images by this procedure. Fig. 3(a) shows a sample image and Fig. 3(b) its eight texturized versions.

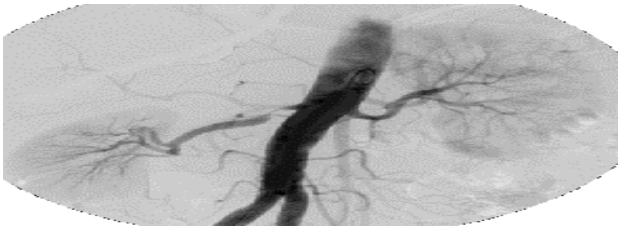

Fig. 3(a): Sample image

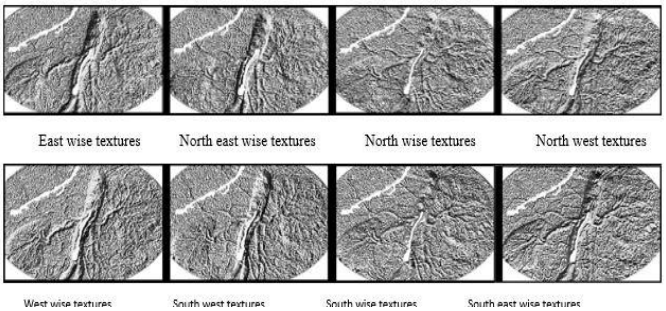

Fig. 3(b): Directional textures of the sample image

C. Skin Images - Morphological Processing

The following 4 points are the definite methodology to complete morphological preparing.

1. The given skin picture is texturized a picked way. One can texturize a given picture in eight potential ways. For this situation, north astute texturization is done for each of the nine skin pictures.
2. Morphological channel 1100 (widening enlargement disintegration) is applied to the texturized picture to identify irregularities in the skin.
3. The sifted picture is dyadically duplicated with the first skin picture
4. The coming about picture intently looks like unique picture however with variations from the norm communicated.

Figs. 4 to 6 show filtered images of all three test case skin images.

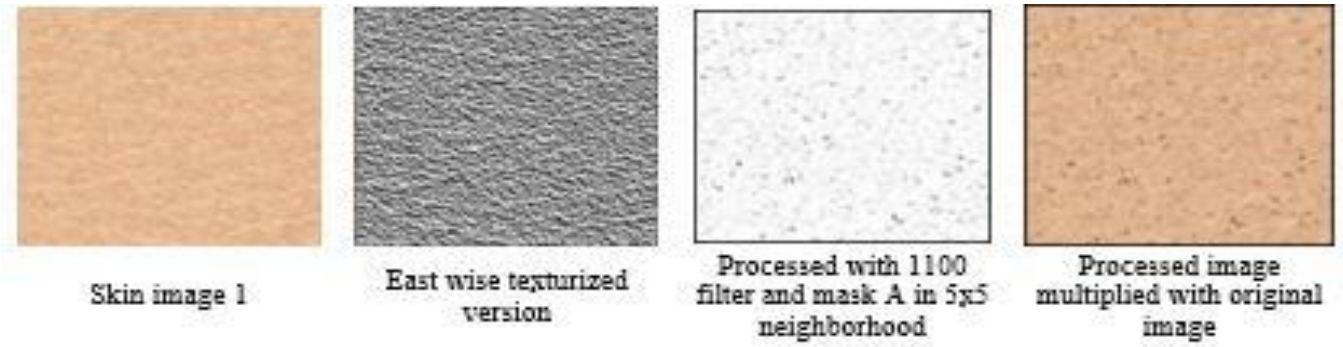

Fig. 4: Skin image 1 and its filtered version

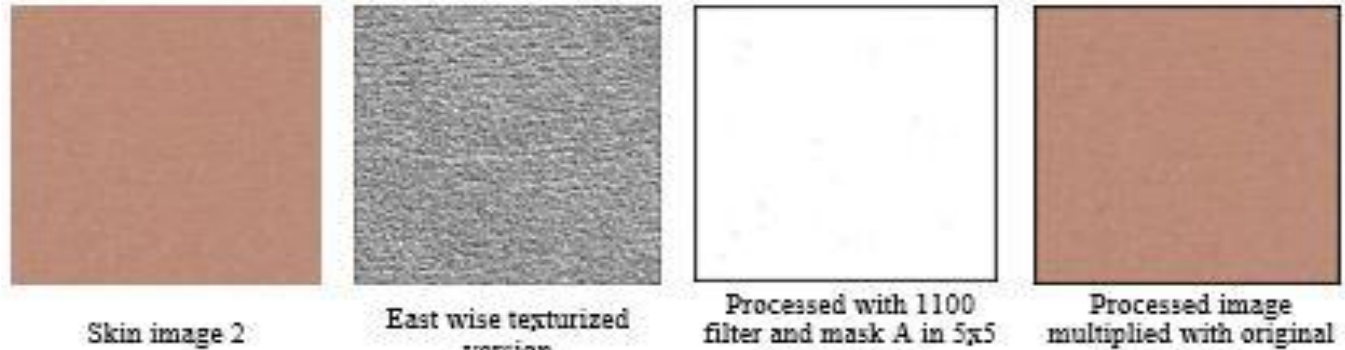

Fig. 5: Skin image 2 and its filtered version

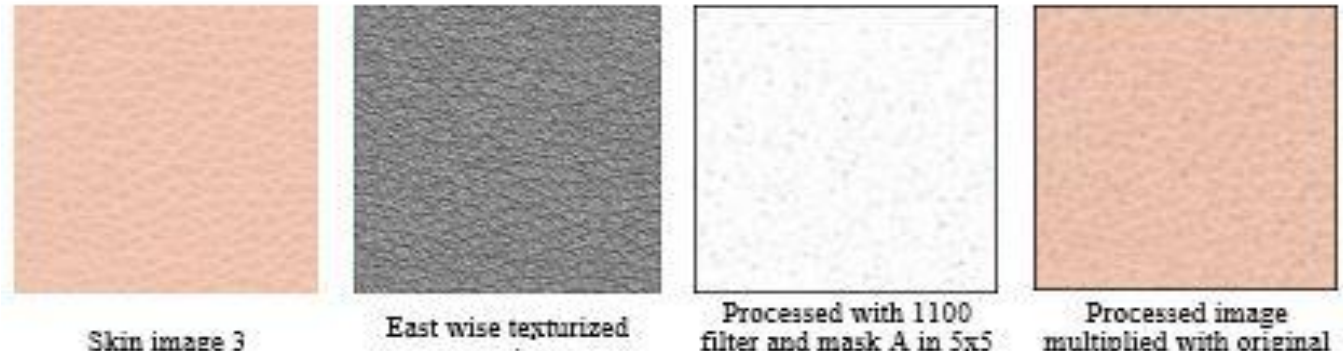

Fig. 6: Skin image 3 and its filtered version

II. CONTEXTUAL ANALYSIS – 1

A. Morphological Filtered Skin Images - Statistical Parameters

The first set of 3 skin pictures are examined by statistical parameters and the outputs are framed in table I. Filtered image 1 shows perceivable skin abnormalities, image 3 shows melanoma content and image 2 does not exhibit any perceivable skin abnormality.

Table I: Statistical parameters for images 1, 2 and 3

Filtered image 1		Filtered image 2		Filtered image 3	
Pixels Count	353847	Pixels Count	290505	Pixels Count	433957
Pixels without black	342027	Pixels without	279825	Pixels without	420877
Red Min	0	Red Min	0	Red Min	0
Red Max	248	Red Max	223	Red Max	255
Red Mean	214.530833948006	Red Mean	179.877382489114	Red Mean	227.512082994398
Red Standard Deviation	41.0647773960355	Red Standard Deviation	35.2887790990204	Red Standard Deviation	40.7257016684497
Red Median	223	Red Median	186	Red Median	234
Red Total Count	353847	Red Total Count	290505	Red Total Count	433957
Green Min	0	Green Min	0	Green Min	0
Green Max	207	Green Max	180	Green Max	240
Green Mean	172.121057971383	Green Mean	133.920176933271	Green Mean	187.176623490346
Green Standard Deviation	33.3672125896639	Green Standard Deviation	26.3825052735597	Green Standard Deviation	34.2795566612662
Green Median	179	Green Median	139	Green Median	191
Green Total Count	353847	Green Total Count	290505	Green Total	433957
Blue Min	0	Blue Min	0	Blue Min	0
Blue Max	174	Blue Max	161	Blue Max	228
Blue Mean	137.44035133829	Blue Mean	115.89930982255	Blue Mean	168.267669377381
Blue Standard Deviation	27.30230083675	Blue Standard Deviation	22.9942230296481	Blue Standard Deviation	31.5655115612477
Blue Median	142	Blue Median	120	Blue Median	171
Blue Total Count	353847	Blue Total Count	290505	Blue Total Count	433957
Saturation Min	0	Saturation Min	0	Saturation Min	0
Saturation Max	0.850980401039124	Saturation Max	0.490196079015732	Saturation Max	1
Saturation Mean	0.533848226070404	Saturation Mean	0.313809990882874	Saturation Mean	0.590187013149261
Saturation Standard Deviation	0.123165272176266	Saturation Standard	0.0625388398766518	Saturation Standard	0.138767182826996

Among all quantitatively measured statistical parameters, the values of the medians of red, green and blue color components are shown in Fig. 7.

Color Medians	Image 1	Image 2	Image 3
Red Median	223	186	234
Green Median	179	139	191
Blue Median	142	120	171

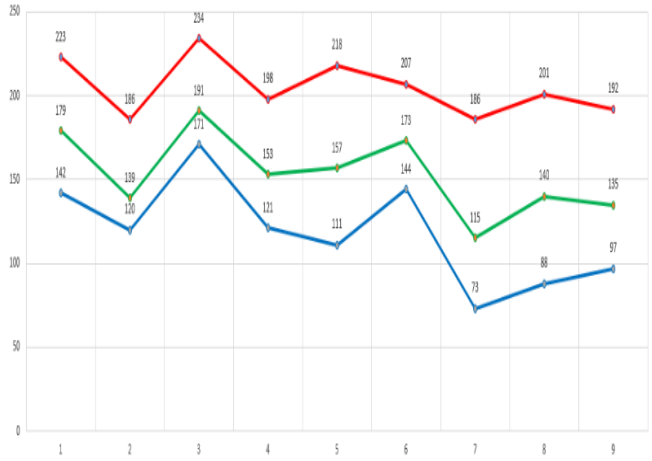

Fig. 7: Color medians of all nine filtered skin images

A total contextual analysis of assessing 'Human Visual Quantization Threshold (HVQT)' based visual quality measure is introduced in the following area.

B. Visual Quality Measures

Table II: Filtered Image 1- Visual Quality Measures

Threshold	Counter	Image Size	Visual Quality	Entropy	|Entropy-Visual Quality|	ToT	HVQT
0	0	353847	0	100	100		
1	6727	353847	1.901104	98.0989	96.19779		
2	6749	353847	1.907322	98.09268	96.18536		
3	7605	353847	2.149234	97.85077	95.70153		
4	12839	353847	3.628404	96.3716	92.74319		
5	27552	353847	7.786416	92.21358	84.42717		
6	52635	353847	14.87507	85.12493	70.24985		
7	85454	353847	24.14999	75.85001	51.70003		
8	121966	353847	34.46857	65.53143	31.06286		
9	158488	353847	44.78998	55.21002	10.42004		
10	192240	353847	54.32857	45.67143	8.657131	10	

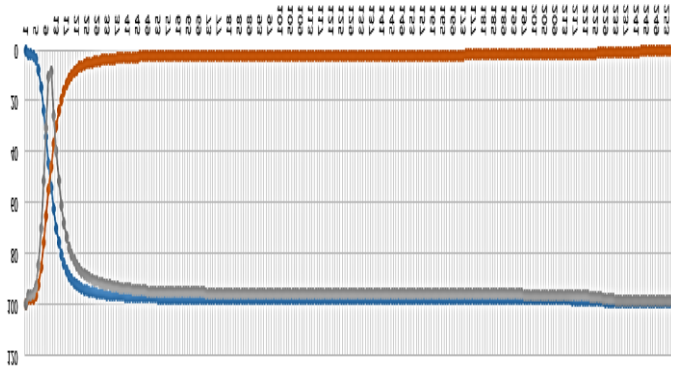

Fig. 8: Graph connecting thresholds and visual quality values for filtered image 1

Table III: Filtered Image 2 - Visual Quality Measures

Threshold	Counter	Image Size	Visual Quality	Entropy	|Entropy-Visual Quality|	ToT	HVQT
0	0	290505	0	100	100		
1	6679	290505	2.2991	97.7009	95.4018		
2	11937	290505	4.109051	95.89095	91.7819		
3	33836	290505	11.6473	88.3527	76.70539		
4	74810	290505	25.75171	74.24829	48.49658		
5	123755	290505	42.59996	57.40004	14.80009	5	
6	168751	290505	58.08885	41.91115	16.17769		
7	204457	290505	70.37986	29.62014	40.75971		7
8	230440	290505	79.32394	20.67606	58.64787		
9	248108	290505	85.40576	14.59424	70.81152		
10	259953	290505	89.48314	10.51686	78.96628		

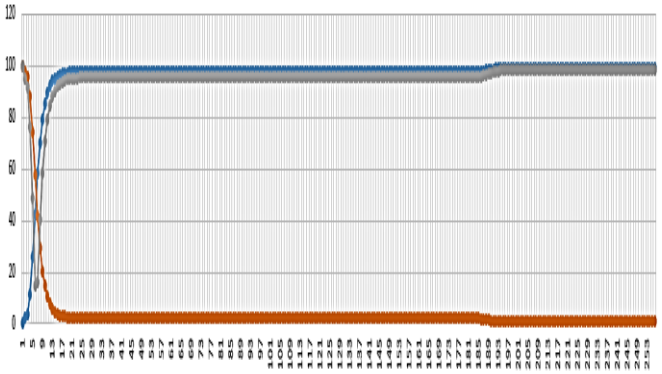

Fig. 9: Graph connecting thresholds and visual quality values for filtered image 2

Table IV: Filtered Image 3 - Visual Quality Measures

Threshold	Counter	Image Size	Visual Quality	Entropy	|Entropy-Visual Quality|	ToT	HVQT
0	0	433957	0	100	100		
1	7402	433957	1.705699	98.2943	96.5886		
2	7417	433957	1.709156	98.29084	96.58169		
3	7724	433957	1.7799	98.2201	96.4402		
4	9762	433957	2.249532	97.75047	95.50094		
5	16230	433957	3.740002	96.26	92.52		
6	29275	433957	6.74606	93.25394	86.50788		
7	48978	433957	11.28637	88.71363	77.42726		
8	73463	433957	16.92864	83.07136	66.14273		
9	100324	433957	23.11842	76.88158	53.76316		
10	127877	433957	29.46767	70.53233	41.06467		

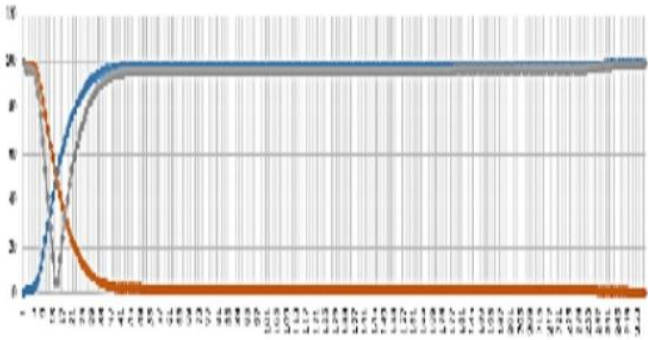

Fig. 10: Graph connecting thresholds and visual quality values for filtered image 3

Table III, IV shows the values of ToT, HVQT and HVQT-ToT. Fig. 11 shows a graph connecting visual quality measures (ToT& HVQT) and all nine filtered skin images.

Table V: All three Morphological Filtered Images - Visual Quality Measures

Visual Quality Measures	Filtered Image 1	Filtered Image 2	Filtered Image 3
ToT	10	5	13
HVQT	14	7	22
HVQT-ToT	4	2	9

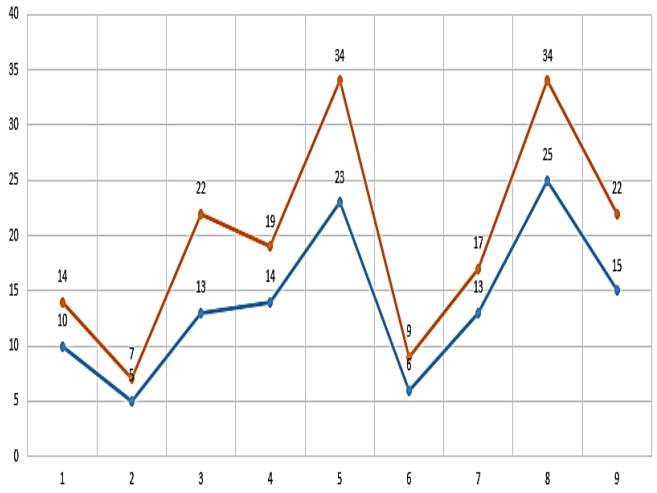

Fig. 11: Graph connecting ToT& HVQT measures and all three filtered images

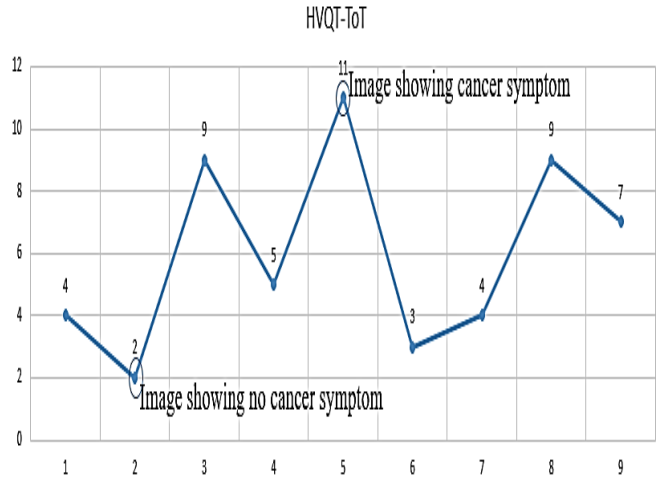

Fig. 12: Graph connecting values of HVQT-ToT and all three filtered skin images

It isn't hard to recognize any indication for skin carcinoma in all the three experiment separated pictures.
Texturization and morphological sifting were applied to the first test pictures and coming about separated pictures inspected for any conceivable side effect of skin carcinoma.
The inquiry that emerges here is that whether it is conceivable to utilize the morphological separating procedure to demonstrate instances of 'bogus positive' and 'bogus negative' choices.

One such instance of 'bogus positive' choice is examined for the Contextual analysis 2.

III. CONTEXTUAL ANALYSIS – 2

A. False Positive Decision

A patient's both ways legs were influenced by some sort of organism and it was expressed that the patient has skin carcinoma in the legs.
Figs. 13.1 and 13.2 separately show the captured pictures of both left and right legs.
An iPhone 6 Plus portable camera was utilized for catching these pictures.

Patient's left leg image	Patient's left leg image equalized

Fig. 13.1: Real time skin image and its equalized version of a patient's left leg

These pictures were morphologically separated and inspected for the presence of skin carcinoma. The outcome ended up being negative, which means the assessment shaped on this patient is a 'bogus positive' choice. Test subtleties are given beneath.

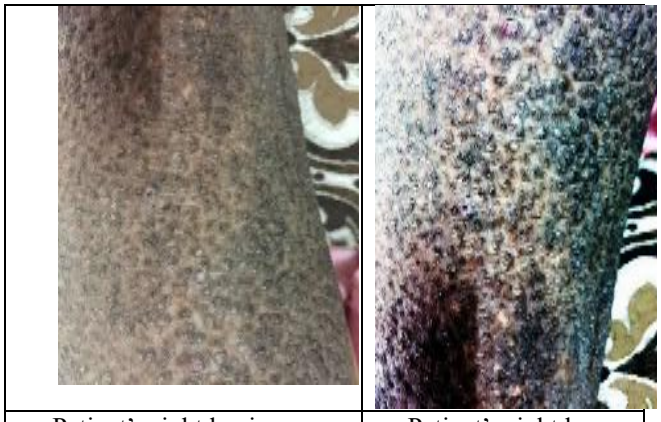

Patient's right leg image	Patient's right leg image equalized

Fig. 13.2: Real time skin image and its equalized version of a patient's right leg

B. Left and Right Leg Skin Images - Statistical Parameters

Table VI: Original images of both legs - Statistical parametric values

			
Original left leg skin image		Original right leg skin image	
Pixels Count	7990272	Pixels Count	7990272
Pixels without black	7990272	Pixels without black	7990272
Red Min	17	Red Min	26
Red Max	255	Red Max	251
Red Mean	140.007143060962	Red Mean	131.830645064398
Red Standard Deviation	28.9024388494293	Red Standard Deviation	34.2618454425707
Red Median	139	Red Median	131
Red Total Count	7990272	Red Total Count	7990272
Green Min	12	Green Min	0
Green Max	255	Green Max	255
Green Mean	129.805218145265	Green Mean	121.786528418557
Green Standard Deviation	29.1945947452379	Green Standard Deviation	36.1137012924896
Green Median	129	Green Median	119
Green Total Count	7990272	Green Total Count	7990272
Blue Min	6	Blue Min	6
Blue Max	255	Blue Max	255
Blue Mean	117.428137990797	Blue Mean	109.919906356129
Blue Standard Deviation	29.5189872885853	Blue Standard Deviation	35.4181565431821
Blue Median	116	Blue Median	105
Blue Total Count	7990272	Blue Total Count	7990272
Saturation Min	0	Saturation Min	0
Saturation Max	1	Saturation Max	1
Saturation Mean	0.113816499710083	Saturation Mean	0.120859831571579
Saturation Standard Deviation	0.0956049412488937	Saturation Standard Deviation	0.0799953788518906

Table VII shows the statistical parametric values of the morphological filtered images of both legs.

Table VII: Statistical parametric values of the filtered images of both legs

	
Morphological filtered left leg skin image	Morphological filtered right leg skin image

Pixels Count	7990272	Pixels Count	7990272
Pixels without black	7918620	Pixels without black	7990272
Red Min	0	Red Min	26
Red Max	255	Red Max	251
Red Mean	136.462064745731	Red Mean	131.830645064398
Red Standard Deviation	30.705175100044	Red Standard Deviation	34.2618454425707
Red Median	136	Red Median	131
Red Total Count	7990272	Red Total Count	7990272
Green Min	0	Green Min	0
Green Max	255	Green Max	255
Green Mean	126.536860947913	Green Mean	121.786528418557
Green Standard Deviation	30.3899048945O8	Green Standard Deviation	36.1137012924896
Green Median	126	Green Median	119
Green Total Count	7990272	Green Total Count	7990272
Blue Min	0	Blue Min	6
Blue Max	255	Blue Max	255
Blue Mean	114.513385401648	Blue Mean	109.919906356129
Blue Standard Deviation	30.244266515124	Blue Standard Deviation	35.4181565431821
Blue Median	114	Blue Median	105
Blue Total Count	7990272	Blue Total Count	7990272
Saturation Min	0	Saturation Min	0
Saturation Max	1	Saturation Max	1
Saturation Mean	0.106276154518127	Saturation Mean	0.120859831571579
Saturation Standard Deviation	0.0696222558617592	Saturation Standard Deviation	0.0799953788518906

Visual quality measures of 'Human Visual Quantization Threshold (HVQT)' based visual quality measure is presented in the next section.

C. Visual Quality Measures

Table VIII: Original Left Leg Image - Visual Quality Measures

Threshold	Counter	Image Size	Visual Quality	Entropy	|Entropy-Visual Quality|	ToT	HVQT
0	0	7990272	0	100	100		
1	10003	7990272	0.12519	99.87481	99.74962		
2	20985	7990272	0.262632	99.73737	99.47474		
3	45538	7990272	0.569918	99.43008	98.86016		
4	121273	7990272	1.517758	98.48224	96.96448		
5	302782	7990272	3.789383	96.21062	92.42123		
6	622760	7990272	7.793977	92.20602	84.41205		
7	1068305	7990272	13.37007	86.62993	73.25986		
8	1602482	7990272	20.05541	79.94459	59.88918		
9	2184422	7990272	27.33852	72.66148	45.32296		
10	2770388	7990272	34.67201	65.32799	30.65598		
11	3342159	7990272	41.82785	58.17215	16.3443		
12	3875166	7990272	48.49855	51.50145	3.002902	12	
13	4365486	7990272	54.63501	45.36499	9.270022		
14	4811240	7990272	60.21372	39.78628	20.42744		
15	5207196	7990272	65.1692	34.8308	30.33839		

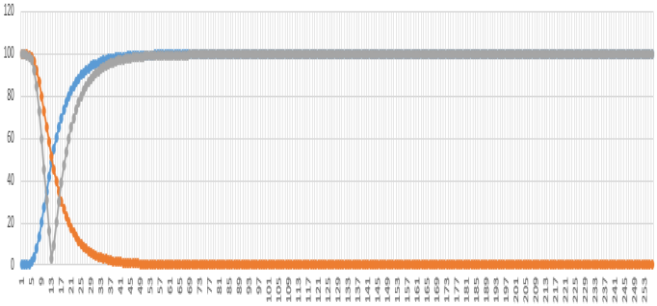

Fig. 14: Graph of thresholds and visual quality values for original left leg image

Table IX: Filtered Left Leg Image - Visual Quality Measures

Threshold	Counter	Image Size	Visual Quality	Entropy	|Entropy-Visual Quality|	ToT	HVQT
0	0	7990272	0	100	100		
1	67526	7990272	0.845103	99.1549	98.30979		
2	91089	7990272	1.139999	98.86	97.72		
3	166233	7990272	2.080442	97.91956	95.83912		
4	337379	7990272	4.222372	95.77763	91.55526		
5	630204	7990272	7.887141	92.11286	84.22572		
6	1040234	7990272	13.01876	86.98124	73.96249		
7	1543220	7990272	19.31374	80.68626	61.37253		
8	2102893	7990272	26.31817	73.68183	47.36367		
9	2685664	7990272	33.61167	66.38833	32.77666		
10	3263107	7990272	40.8385	59.1615	18.32301		
11	3813238	7990272	47.72351	52.27649	4.552986	11	
12	4323957	7990272	54.11527	45.88473	8.230533		
13	4788283	7990272	59.92641	40.07359	19.85282		
14	5205094	7990272	65.14289	34.85711	30.28578		
15	5572392	7990272	69.7397	30.2603	39.47941		

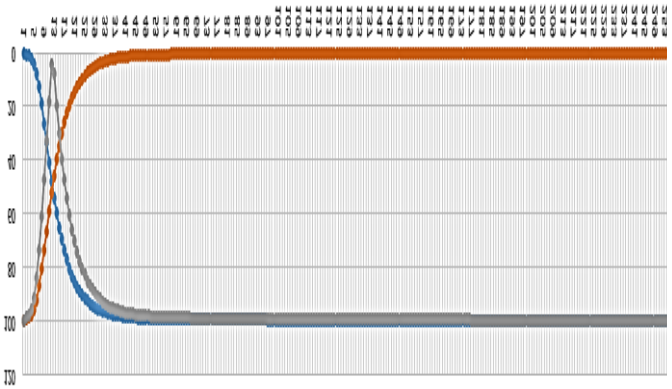

Fig. 15: Graph of thresholds and visual quality values for filtered left leg image

Table X: Original Right Leg Image - Visual Quality Measures

Threshold	Counter	Image Size	Visual Quality	Entropy	|Entropy-Visual Quality|	ToT	HVQT
0	0	7990272	0	100	100		
1	21669	7990272	0.271192	99.72881	99.45762		
2	77851	7990272	0.974322	99.02568	98.05136		
3	224794	7990272	2.813346	97.18665	94.37331		
4	508148	7990272	6.359583	93.64042	87.28083		
5	929458	7990272	11.63237	88.36763	76.73526		
6	1465731	7990272	18.34394	81.65606	63.31211		
7	2074607	7990272	25.96416	74.03584	48.07168		
8	2713799	7990272	33.96379	66.03621	32.07243		
9	3346832	7990272	41.88633	58.11367	16.22733		
10	3951091	7990272	49.44877	50.55123	1.102466	10	
11	4507659	7990272	56.41434	43.58566	12.82867		
12	5007717	7990272	62.67267	37.32733	25.34534		
13	5453562	7990272	68.25252	31.74748	36.50504		
14	5840624	7990272	73.09669	26.90331	46.19337		
15	6174865	7990272	77.27978	22.72022	54.55957		
16	6460227	7990272	80.85115	19.14885	61.70231		16

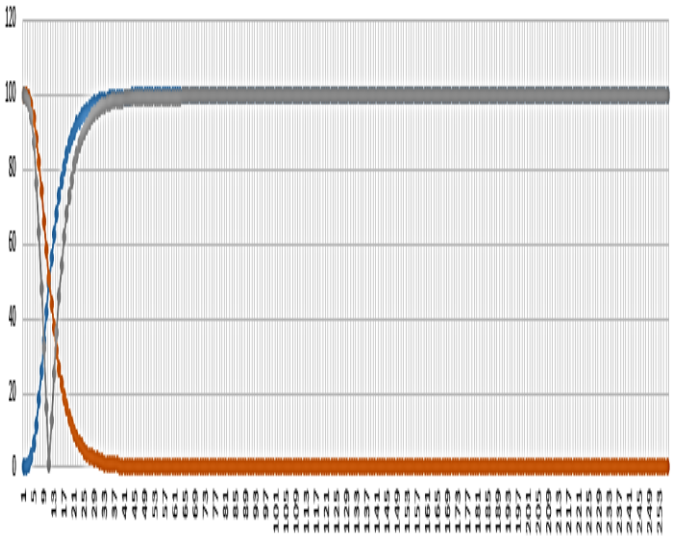

Fig. 16: Graph of thresholds and visual quality values for original right leg image

Table XI: Filtered Right Leg Image - Visual Quality Measures

Threshold	Counter	Image Size	Visual Quality	Entropy	|Entropy-Visual Quality|	ToT	HVQT
0	0	7990272	0	100	100		
1	579	7990272	0.007246	99.99275	99.98551		
2	6969	7990272	0.087219	99.91278	99.82556		
3	47890	7990272	0.599354	99.40065	98.80129		
4	184996	7990272	2.315265	97.68473	95.36947		
5	474947	7990272	5.944065	94.05593	88.11187		
6	926492	7990272	11.59525	88.40475	76.8095		
7	1491019	7990272	18.66043	81.33957	62.67914		
8	2121827	7990272	26.55513	73.44487	46.88974		
9	2760466	7990272	34.54784	65.45216	30.90433		
10	3379106	7990272	42.29025	57.70975	15.4195		
11	3962691	7990272	49.59394	50.40606	0.812113	11	
12	4490901	7990272	56.20461	43.79539	12.40921		
13	4966847	7990272	62.16118	37.83882	24.32235		
14	5391011	7990272	67.46968	32.53032	34.93936		
15	5753690	7990272	72.00869	27.99131	44.01738		
16	6076481	7990272	76.04849	23.95151	52.09697		16

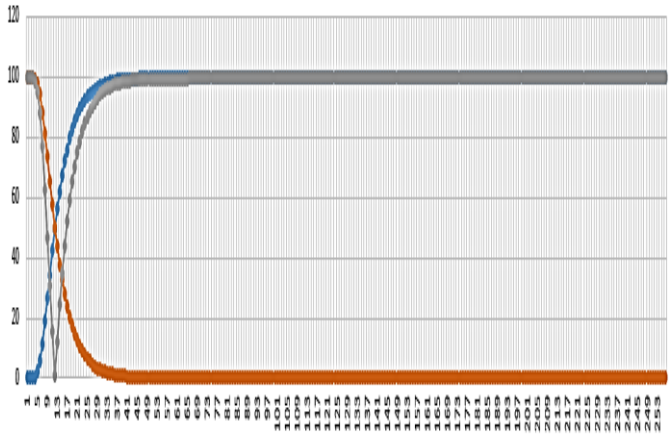

Fig. 17: Graph of thresholds and visual quality values for filtered right leg image

IV. RESULTS AND OBSERVATIONS

Table X shows the values of ToT, HVQT and HVQT-ToT. Fig. 17 shows a graph connecting visual quality measures (ToT & HVQT) and both the original and the filtered skin images.

Table XII: All Three Morphological Filtered Images - Visual Quality Measures

Visual Quality Measures	Left leg original image	Filtered left leg image	Right leg original image	Filtered right leg image
ToT	12	11	10	11
HVQT	18	18	16	16
HVQT-ToT	6	7	6	5

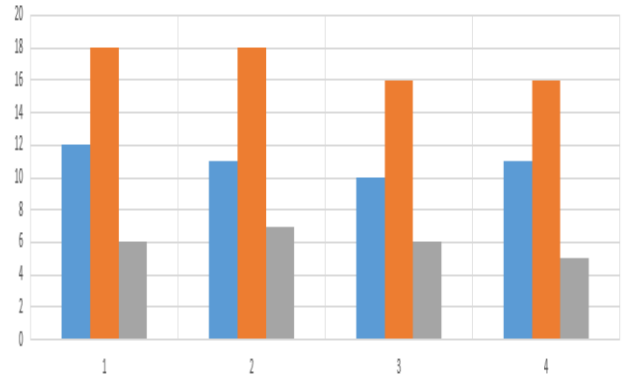

Fig. 18: Graph connecting visual quality measures and leg skin images

Since the HVQT-ToT esteems remain nearly the equivalent (5, 6 and 7), the leg skin pictures don't represent any danger of skin carcinoma. Along these lines, the choice made on this present patient's skin status is seen here as **'FALSE POSITIVE DECISION'.** The skin is influenced by 'organism' or might be by 'neurological dermatitis'.

V. CONCLUSION

1. All skin pictures are practically white adjusted since factual parametric qualities continue as before for the instances of typical and WB shading portrayals.
2. Skin picture 3 shows plausibility of skin carcinoma among every one of the three sifted pictures.
3. Skin picture 2 is the best among each of the three separated pictures.
4. Reviewing of skin quality should be possible dependent on the estimations of (HVQT – ToT)
5. Both the skin pictures of left and right legs are practically white adjusted since measurable parametric qualities remain nearly the equivalent for the instances of ordinary and WB shading portrayals.
6. Both skin pictures show probability of organism development and not skin carcinoma.
7. Evaluating of skin quality should be possible dependent on the estimations of (HVQT – ToT)

REFERENCES

1. Dana, K. J., van Ginneken, B., Nayar, S. K., and Koenderink, J. J., 1999, "Reflectance and texture of real world surfaces", ACM Transactions on Graphics **18(1)**, 1–34
2. DeCarlo, D., Metaxas, D., and Stone, M., 1998, "An anthropometric face model using variational techniques", 27 Proceedings of SIGGRAPH 67–74
3. Dong, J. and Chantler, M., 2002, "Capture and synthesis of 3D surface texture", Proceedings of Texture 2002 - The 2nd international workshop on texture analysis and synthesis 41–46
4. Guenter, B., Grimm, C.,Wood, D., Malvar, H., and Pighin, F., 1998, "Making faces", Proceedings of SIGGRAPH 55–66
5. Ishii, T., Yasuda, T., Yokoi, S., and Toriwaki, J., 1993, "A generation model for human skin texture", Communicating with Virtual Worlds , pp. 139–150
6. Jain, A., Prabhakar, S., and Hong, L., 1999, "A multichannel approach to fingerprint classification", IEEE Transactions on Pattern Analysis and Machine Intelligence **21(4)**, 348–369
7. Julesz, B., 1981, "Textons, the elements of texture perception and their interactions", Nature **(290)**, 91–97 Koenderink, J. J. and van Doorn, A. J., 1996, "Illuminance texture due to surface mesostructure", Journal of the Optical Society of America A **13(3)**, 452–63
8. Koenderink, J. J., van Doorn, A. J., Dana, K. J., and Nayar, S. K., 1999, "Bidirectional reflection distribution function of thoroughly pitted surfaces", International Journal of Computer Vision **31(2-3)**, pp. 129–144
9. Lee, Y., Terzopoulos, D., and Walters, K., 1995, "Realistic modeling for facial animation", Proceedings of SIGGRAPH 55–62
10. Leung, T. and Malik, J., 1999, "Recognizing surfaces using three-dimensional textons", International Conference on Computer Vision **2**, 1010–1017
11. Leung, T. and Malik, J., 2001, "Representing and recognizing the visual appearance of materials using three dimensional textons", International Journal of Computer Vision **43(1)**, 29–44
12. Liu, X., Yu, Y., and Shum, H., 2001, "Synthesizing bidirectional texture functions for real-world surfaces", Proceedings of SIGGRAPH 97–106
13. Ma, W. Y. and Manjunath, B. S., 1996, "Texture features and learning similarity", Proceedings of the IEEE Conference on Computer Vision and Pattern Recognition 425–430
14. McGunnigle, G. and Chantler, M. J., 2000, "Rough surface classification using first order statistics from photometric stereo", Pattern Recognition Letters **21**, 593–604
15. Murase, H. and Nayar, S. K., 1995, "Visual learning and recognition of 3-D objects from appearance", International Journal of Computer Vision 5–24
16. Nahas, M., Huitric, H., Rioux, M., and Domey, J., 1990, "Facial image synthesis using skin texture recording", Visual Computer **6(6)**, pp. 337–43.
17. Penirschke, A., Chantler, M., and Petrou, M., 2002, "Illuminant rotation invariant classification of 3D surface 28 textures using Lissajous's ellipses", Proceedings of Texture 2002 - The 2nd international workshop on texture analysis and synthesis , pp. 103–108
18. Pont, S. C. and Koenderink, J. J., 2002, "Bidirectional texture contrast function", Proceedings of the European Conference on Computer Vision 2353(IV), pp. 808–822

AUTHORS PROFILE

S. Sree Hari Raju, completed his M.Tech Computer Science & Engineering and pursuing Ph.D from University of Mysore. His area of interest is in Image Processing, AI, Data Mining, Machine Learning.

Dr. E G Rajan, done his Ph.D form IIT-Kanpur. His area of interest is in Signal and Image Processing, Data Mining, Machine Learning.